Editors' Suggestion | Featured in Physics

Membraneless Phonon Trapping and Resolution Enhancement in Optical Microwave Kinetic Inductance Detectors

Nicholas Zobrist,[1,*] W. Hawkins Clay,[1] Grégoire Coiffard,[1] Miguel Daal,[1] Noah Swimmer,[1] Peter Day,[2] and Benjamin A. Mazin[1]

[1]Department of Physics, University of California, Santa Barbara, California 93106, USA
[2]Jet Propulsion Laboratory, California Institute of Technology, Pasadena, California 91125, USA

(Received 14 December 2021; revised 22 February 2022; accepted 18 May 2022; published 1 July 2022)

Microwave kinetic inductance detectors (MKIDs) sensitive to light in the ultraviolet to near-infrared wavelengths are superconducting microresonators that are capable of measuring photon arrival times to microsecond precision and estimating each photon's energy. The resolving power of nonmembrane MKIDs has remained stubbornly around 10 at 1 μm despite significant improvements in the system noise. Here we show that the resolving power can be roughly doubled with a simple bilayer design without needing to place the device on a membrane, avoiding a significant increase in fabrication complexity. Based on modeling of the phonon propagation, we find that the majority of the improvement comes from the inability of high energy phonons to enter the additional layer due to the lack of available phonon states.

DOI: 10.1103/PhysRevLett.129.017701

To directly image an exoplanet and spectrally characterize its atmosphere, detectors sensitive to light in the 400 nm to 2.5 μm wavelength range are crucial. Superconducting sensors are important candidates for this application since the low gap energy Δ allows for the detection of individual photons. Compared with semiconducting options, superconducting sensors count photons with essentially no noise. This property helps overcome the challenge of the extremely low light levels received from exoplanets [1,2]. Additionally, in this range of photon wavelengths there are several important spectral features associated with habitability and life which set the required detector performance [3]. Recommendations for this application in an integral field spectrograph (IFS) typically specify a resolving power of $R = E/\delta E \sim 100$, where δE is the full-width half-maximum energy resolution of the device at the photon energy E [4]. However, for space-based instruments where the Earth's atmosphere does not interfere, resolving powers as low as 25 can identify large molecular absorption bands like those of water [5].

Several superconducting detector technologies have been proposed for imaging at these wavelengths. Among them are transition edge sensors [6–8] and superconducting tunnel junctions [9,10]. However, for an exoplanet IFS tens of thousands to millions of pixels are required to cover the desired field of view which introduces significant wiring challenges in the cryogenic device environment. Microwave kinetic inductance detectors (MKIDs) natively solve this issue and achieve similar spectral resolution. Each sensor is a microwave resonator whose inductance and loss temporarily increase after the absorption of a photon [11]. Photon energies can then be determined by probing each pixel at its resonance frequency and measuring the size of its photon response. This design allows for the straightforward frequency multiplexing of up to 2 000 pixels per feedline and has enabled the demonstration of arrays of up to 20 000 pixels [12,13].

The limiting resolving power of optical MKIDs is set by the interaction between broken Cooper pairs, also known as quasiparticles, and phonons in the superconductor. The two systems are coupled, and as the energy down-converts from the initial photon absorption, roughly 41% of the initial energy will be contained in phonons with energies below 2Δ at which point they can no longer break new Cooper pairs and be detected [14]. The exact amount of energy lost in this manner is statistical and sets the maximum achievable resolving power, called the Fano limit [15]:

$$R_{\mathrm{Fano}} = \frac{1}{2\sqrt{2\ln(2)}}\sqrt{\frac{\eta_{\mathrm{pb}}E}{\Delta F}}. \tag{1}$$

Here, η_{pb} and F are the pair breaking efficiency and the Fano factor. We use the standard values 0.59 [14] and 0.2 [16,17] respectively for each since they are difficult to measure and vary only weakly across most superconductors [14,15]. For a detector with a superconducting transition at 500 mK, the Fano limit gives a maximum resolving power of roughly 59 at 2.5 μm and 147 at 400 nm, right in the target range for an exoplanet IFS.

In practice, achieving the Fano limit in real detectors has proven difficult. Phonons escaping into the substrate before they fall below the 2Δ energy threshold can significantly reduce the observed resolving power [18–20]. We account

for this excess loss by introducing an extra phonon loss factor J into Eq. (1) [21]:

$$R_{\text{phonon}} = \frac{1}{2\sqrt{2\ln(2)}}\sqrt{\frac{\eta_{\text{pb}}E}{\Delta(F+J)}}. \quad (2)$$

After measuring the signal-to-noise contribution to the resolving power R_{noise}, the total resolving power is given as $1/R^2 = 1/R^2_{\text{noise}} + 1/R^2_{\text{phonon}}$. In this way, J can be estimated for different materials and geometries assuming that there are no other contributions to R. The photon event absorption position along with a nonuniform current density in the inductor can also contribute to a decreased resolving power, but modeling of these effects suggests that they do not contribute significantly to this design as long as $R \lesssim 40$ [20].

The best published MKID resolving powers to date have been in NbTiN-Al hybrid coplanar waveguide resonators suspended on silicon nitride membranes [19]. Compared to that of a device on a thick substrate, the membrane device had a higher resolving power, corresponding to a decrease in J by a factor of about 8, from 3.1 to 0.38. The much thinner membrane allows partially escaped phonons to be quickly recollected in the sensor before reaching the substrate. The extra chance to down-convert into quasiparticles and be detected increases the average time required for phonons to fully escape, τ_{esc}, and results in a higher resolving power. This improvement was shown to be consistent with a simple geometric ray-tracing phonon model, which used the proportionality of J to the ratio between the phonon pair breaking time and the escape time $\tau_{\text{pb}}/\tau_{\text{esc}}$ to evaluate the expected decrease in J.

While the membrane devices give an impressive increase in R, they introduce significant fabrication complexity. Additionally, the aluminum sensor used in that demonstration is small, highly reflective of optical photons, and has a low kinetic inductance, which makes it difficult to create large arrays with high quantum efficiency. A more realistic detector design for a kilo- or megapixel detector requires a more disordered superconductor with a higher kinetic inductance that can be patterned into a compact lumped element circuit like shown in Fig. 1. The lumped element design allows for light to be focused onto the inductor with a microlens array making fill factors of $> 90\%$ possible. Hafnium has proven to be the best material out of the higher inductance materials tested so far [13,22] and has the added benefit of being much less reflective than aluminum [23,24]. We present a measurement of the resolving power of a 220 nm thick hafnium detector on a sapphire substrate with a superconducting transition temperature of $T_c = 395$ mK, in Fig. 2. More details on the resolving power calculation can be found in the Supplemental Material [25], which uses Refs. [26,27]. The breakdown of the noise contributions to R shows that athermal phonon escape is the leading factor for the tested

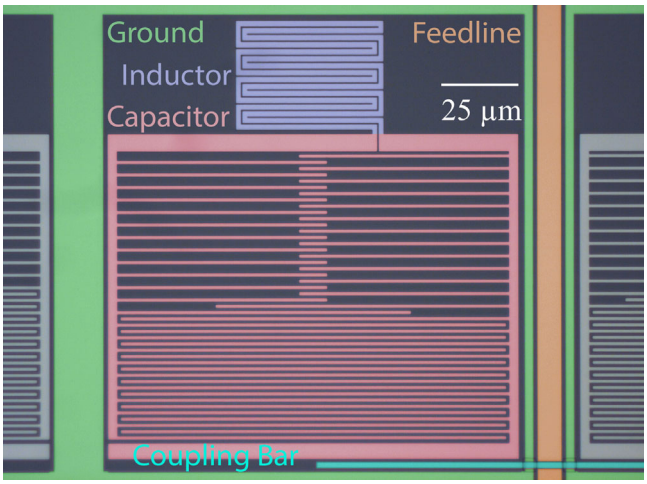

FIG. 1. A microscope image of a hafnium optical kinetic inductance detector coupled to a coplanar waveguide feedline. The image has been given false color to highlight the functions of each part of the device. The dark areas are the bare sapphire substrate. Light is focused onto the 47 μm $\times$ 34.7 μm inductor with a microlens, which allows arrays of these detectors to achieve near unity fill factors. An approximate scale bar is included for reference.

energy range, corresponding to $J = 13$. This value for J is larger than that for aluminum on silicon nitride, but because of hafnium's lower gap energy, the limiting resolving power is similar.

To decrease J without a membrane, some form of a phonon blocking layer must be introduced between the photosensitive superconductor and substrate. This layer may take the form of a material with an acoustic impedance very different from either the substrate or sensor material. In this case, phonons would preferentially be reflected back into the sensor allowing for more opportunities to break Cooper pairs into quasiparticles before falling below the 2Δ threshold. An example of this kind of layer might be a low density polymer like polymethyl methacrylate (PMMA), which according to the acoustic mismatch model would reduce the effective phonon transmission coefficient into the sapphire by a factor of 3.1 [28,29]. See the Supplemental Material [25] for more details on the acoustic mismatch calculation which uses Refs. [30,31].

However, amorphous-insulating blocking layers like PMMA are another potential source of loss and should be kept away from the MKID capacitor to avoid excess two-level system noise [32]. Since most of the escaping phonons contributing to J have energies near the Debye energy of the sensor material, a potential alternative, then, is to find a metallic (preferably superconducting) layer that has a low enough density and speed of sound to not have any available phonon states near that energy. Out of the available elemental superconductors, indium stands out as one of the softest. Indium's effective phonon cutoff energy is much lower than that of hafnium: the Debye temperature

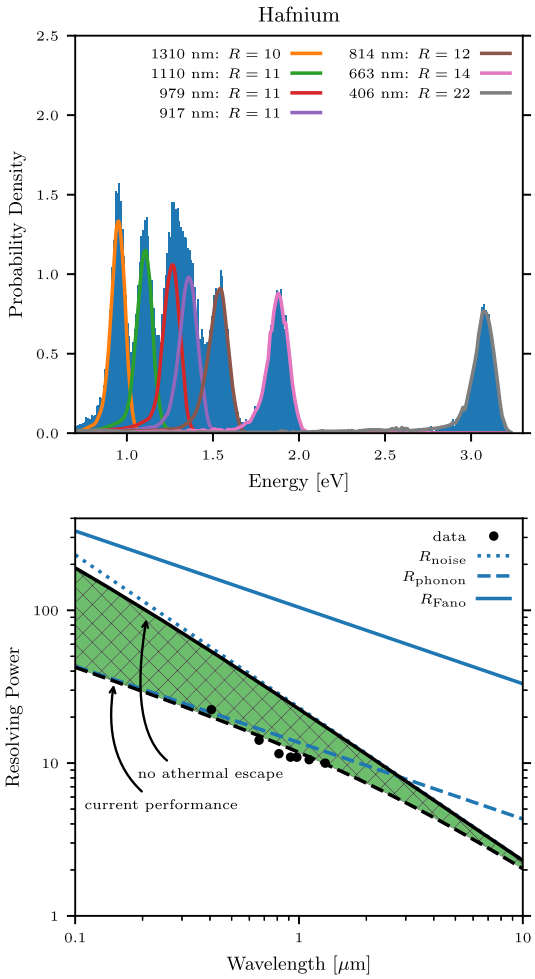

FIG. 2. Top: plotted are the combined spectra for the single layer hafnium device at seven laser energies. The small low energy tail to each distribution is likely explained by quasiparticle diffusion into the insensitive capacitor. Bottom: The noise decomposition for this device is shown. The filled in green area represents the resolving powers achievable by reducing the phonon loss but keeping the same noise spectrum.

of indium, 112 K, is roughly half of that in hafnium, 252 K [33]. Unlike with PMMA, adding an indium interface layer would result in only a ∼18% decrease in the effective transmission coefficient according to the acoustic mismatch model. The highest energy phonons produced in the hafnium, though, should be unable to escape into the indium below. These phonons have a wavelength on the order of the hafnium lattice spacing, ∼0.3 nm, so indium films that are tens of nanometers thick should provide an effective barrier.

Similar types of multilayers with mismatched Debye temperatures have been previously fabricated to produce low thermal conductivity films at room temperature [34]. Because at higher temperatures the contribution of Debye phonons is important, these systems are effective at limiting the quasiequilibrium heat transfer across the film boundary.

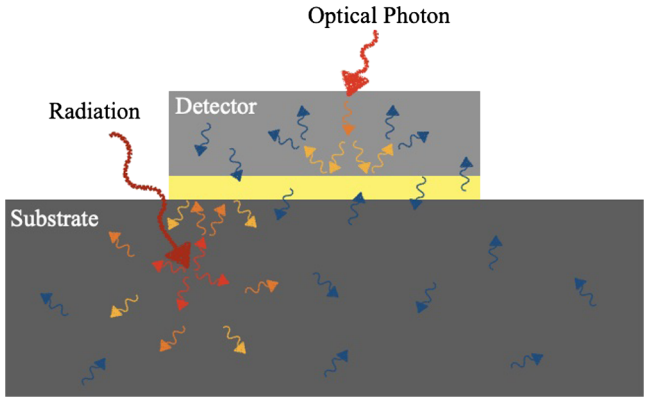

FIG. 3. A schematic representation is shown of the phonon blocking layer (yellow) employed in this paper. The lack of available phonon states in the blocking layer prohibits high energy phonons (red and orange) generated during a photon absorption from escaping the detector material, allowing all of their energy to be measured. Lower energy phonons (blue) pass through the barrier freely. Similarly, the phonon blocking layer provides some protection to the detector from high energy, ionizing radiation absorbed in the substrate.

Work with these multilayers shows that the simple considerations used here to choose an interface material are likely inadequate for fully describing the phonon transport. The fundamental properties of the phonons, for example, are altered from those in a crystal by the amorphous nature of these films and the presence of the interface [35]. However, we will continue to use these simple models as order of magnitude estimates, noting that the future design of this kind of interface layer would benefit from a more detailed analysis.

To demonstrate the phonon blocking effect, we fabricated a hafnium/indium bilayer MKID on silicon, schematically shown in Fig. 3. Silicon was chosen as a substrate to encourage more uniform indium films, but we note that thin layers of indium can be deposited on sapphire if the substrate is cooled to liquid nitrogen temperatures [36]. The tested bilayer was composed of a 15 nm layer of indium with 220 nm of hafnium on top. More fabrication details for this device can be found in the Supplemental Material [25]. We measure $T_c = 468$ mK for hafnium on silicon and 786 mK for the bilayer on silicon. Because of the relatively thin indium layer, we expect the film to be proximitized to a single gap energy with a single superconducting transition temperature. However, the increase in T_c is likely mostly due to fabrication differences instead of the proximity effect [37,38]. See the Supplemental Material [25] for more details. Resonators patterned out of this material had internal quality factors of up to 250 000, which are similar to the quality factors achieved in hafnium alone [23].

Additionally, we found that the quasiparticle lifetime increased when the indium was added, giving a phase and dissipation lifetime of 404 μs and 106 μs for the hafnium device and 452 μs and 401 μs for the bilayer. These values

represent the maximum quasiparticle lifetime at zero quasiparticle density and were found by fitting the detector response decay to a quasiparticle recombination model [39]. More details can be found in the Supplemental Material [25]. The lifetime in the dissipation signal changes the most, which we suspect may be attributable to the higher phonon density inhibiting quasiparticle relaxation into localized, dissipationless states.

Figure 4 shows a dramatic improvement in the resolving power from 11 to 20 at 1 μm in the bilayer devices. From this data, we calculate $J = 1.6$ corresponding to a 8 times improvement in phonon trapping over the original device, similar to the improvement seen by suspending an MKID on a membrane. The full noise breakdown of this device is also shown in Fig. 4 and has been extrapolated to higher and lower wavelengths as a guide to how these detectors are likely to perform outside the tested wavelength range. For the bilayer device above 1 μm, the resolving power is strongly limited by the signal to noise of the photon pulse,

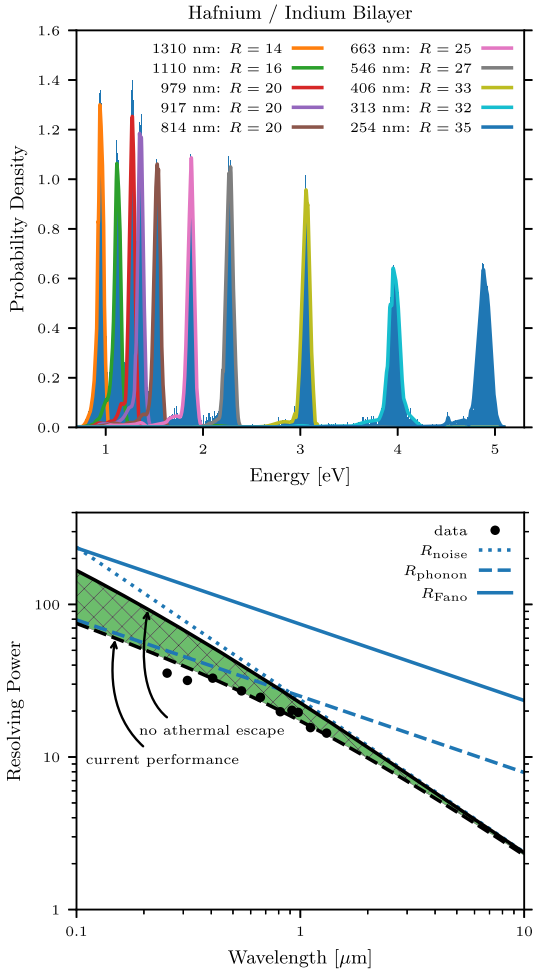

FIG. 4. The combined spectra and noise decomposition for the bilayer device are shown, similar to that in Fig. 2. We see a large improvement in the resolving power which is explained by significantly less athermal phonon escape.

while below 1 μm phonon escape becomes the limiting term in the resolving power.

If the increase in energy resolution were from only the acoustic mismatch introduced by the indium layer, we could compute the expected increase in R using the phonon ray-tracing model developed in Ref. [19]. This model is discussed in more detail in the Supplemental Material [25]. We find that $\tau_{esc} = 12$ ns for hafnium on sapphire and 12 ns for the bilayer on silicon. The ratio of J in the hafnium film to that in the bilayer is given by

$$\frac{J_{Hf}}{J_{Bi}} = \frac{\tau_{esc,Bi}}{\tau_{esc,Hf}} \sim 1. \tag{3}$$

There is effectively no change which is consistent with the similar effective transmission between the two devices. With the higher gap energy in the bilayer, these results suggest that the bilayer should have worse resolving power than that of the hafnium device. Since this is not the case, we infer that an alternative mechanism must be preventing phonon transmission. In the Supplemental Material [25], which uses Refs. [40,41], the size of the phonon trapping effect caused by the lack of high energy phonon states in indium is estimated to reduce J by between 1.7 and 26 which is consistent with our measurements. The uncertainty in this estimation is dominated by the unknown material constants for hafnium.

In conclusion, we have fabricated an optical MKID made out of an indium/hafnium bilayer. We find that the resolving power of this device is nearly twice what has been previously measured in other single layer devices and approaches the best resolving powers measured in membrane suspended MKIDs by achieving a similar amount of phonon trapping. Simulations of the phonon propagation across the extra interface layer do not adequately explain the improved resolving power, and order of magnitude estimates of the energy down-conversion physics point to the low phonon cutoff energy in indium as the primary phonon trapping mechanism. These results show that the simple addition of an extra layer to the MKID sensor material can significantly improve the detector performance, approaching the minimum requirements for an effective exoplanet IFS. Additionally, while the motivation of this letter was focused on exoplanet instrumentation, this technique may reduce the fabrication complexity of detectors where $R \sim 20$ at 1 μm is acceptable, like for bioanalysis research [6] or for dark matter detection [42]. Further improvements to the resolving power in optical MKIDs may involve testing different interface materials or combining the membrane suspension and phonon trapping layer techniques.

The low Debye energy interface layer demonstrated here is an interesting tool for manipulating phonon dynamics at low temperatures and may also have uses in other types of devices. As shown in Fig. 3, it acts as a selective valve,

preventing highly nonequilibrium phonons from crossing the barrier, while allowing passage for low energy phonons which help keep the device in thermal equilibrium with the substrate. We use it here to keep high energy phonons inside of our detector, but the interface layer should also provide protection to the device from absorbing high energy phonons generated in the substrate. One potential source of these phonons is from ionizing radiation, like cosmic rays, which cause detector glitches and lead to a significant increase in dead time in superconducting bolometers [43]. These types of events also pose problems for quantum computers by destroying qubit coherence and increasing error rates [44–46]. This issue may be partially mitigated by implementing a similar interface layer in these respective devices.

N. Z. was supported throughout this work by a NASA Space Technology Research Fellowship. This material is based upon work supported by the National Aeronautics and Space Administration under Grant No. 80NSSC1 9K0329.

*nzobrist@physics.ucsb.edu

[1] A. B. Walter *et al.*, The MKID exoplanet camera for Subaru SCExAO, Publ. Astron. Soc. Pac. **132**, 125005 (2020).
[2] S. Steiger *et al.*, SCExAO/MEC and CHARIS discovery of a low-mass, 6 au separation companion to HIP 109427 using stochastic speckle discrimination and high-contrast spectroscopy, Astron. J. **162**, 44 (2021).
[3] B. J. Rauscher, E. R. Canavan, S. H. Moseley, J. E. Sadleir, and T. Stevenson, Detectors and cooling technology for direct spectroscopic biosignature characterization, J. Astron. Telesc. Instrum. Syst. **2**, 041212 (2016).
[4] The LUVOIR Team, The LUVOIR Mission Concept Study Final Report, arXiv:1912.06219.
[5] J. Wang, D. Mawet, G. Ruane, R. Hu, and B. Benneke, Observing exoplanets with high dispersion coronagraphy. I. The scientific potential of current and next-generation large ground and space telescopes, Astron. J. **153**, 183 (2017).
[6] K. Niwa, T. Numata, K. Hattori, and D. Fukuda, Few-photon color imaging using energy-dispersive superconducting transition-edge sensor spectrometry, Sci. Rep. **7**, 45660 (2017).
[7] J. Burney, T. Bay, J. Barral, P. Brink, B. Cabrera, J. Castle, A. Miller, S. Nam, D. Rosenberg, R. Romani, and A. Tomada, Transition-edge sensor arrays for UV-optical-IR astrophysics, Nucl. Instrum. Methods Phys. Res., Sect. A **559**, 525 (2006).
[8] R. W. Romani, a. J. Miller, B. Cabrera, S. W. Nam, and J. M. Martinis, Phase-resolved crab studies with a cryogenic transition-edge sensor spectrophotometer, Astrophys. J. **563**, 221 (2001).
[9] P. Verhoeve, D. Martin, R. Hijmering, J. Verveer, A. van Dordrecht, G. Sirbi, T. Oosterbroek, and A. Peacock, S-Cam 3: Optical astronomy with a STJ-based imaging spectrophotometer, Nucl. Instrum. Methods Phys. Res., Sect. A **559**, 598 (2006).
[10] D. D. E. Martin, P. Verhoeve, A. Peacock, A. G. Kozorezov, J. K. Wigmore, H. Rogalla, and R. Venn, Resolution limitation due to phonon losses in superconducting tunnel junctions, Appl. Phys. Lett. **88**, 123510 (2006).
[11] P. K. Day, H. G. LeDuc, B. A. Mazin, A. Vayonakis, and J. Zmuidzinas, A broadband superconducting detector suitable for use in large arrays, Nature (London) **425**, 817 (2003).
[12] P. Szypryt, S. R. Meeker, G. Coiffard, N. Fruitwala, B. Bumble, G. Ulbricht, A. B. Walter, M. Daal, C. Bockstiegel, G. Collura, N. Zobrist, I. Lipartito, and B. A. Mazin, Large-format platinum silicide microwave kinetic inductance detectors for optical to near-IR astronomy, Opt. Express **25**, 25894 (2017).
[13] N. Zobrist, G. Coiffard, B. Bumble, N. Swimmer, S. Steiger, M. Daal, G. Collura, A. B. Walter, C. Bockstiegel, N. Fruitwala, I. Lipartito, and B. A. Mazin, Design and performance of hafnium optical and near-IR kinetic inductance detectors, Appl. Phys. Lett. **115**, 213503 (2019).
[14] A. G. Kozorezov, A. F. Volkov, J. K. Wigmore, A. Peacock, A. Poelaert, and R. den Hartog, Quasiparticle-phonon downconversion in nonequilibrium superconductors, Phys. Rev. B **61**, 11807 (2000).
[15] U. Fano, Ionization yield of radiations. II. The fluctuations of the number of ions, Phys. Rev. **72**, 26 (1947).
[16] M. Kurakado, Possibility of high resolution detectors using superconducting tunnel junctions, Nucl. Instrum. Methods Phys. Res. **196**, 275 (1982).
[17] N. Rando, A. Peacock, A. van Dordrecht, C. Foden, R. Engelhardt, B. Taylor, P. Gare, J. Lumley, and C. Pereira, The properties of niobium superconducting tunneling junctions as X-ray detectors, Nucl. Instrum. Methods Phys. Res., Sect. A **313**, 173 (1992).
[18] A. G. Kozorezov, J. K. Wigmore, D. Martin, P. Verhoeve, and A. Peacock, Phonon noise in thin metal films in an advanced energy down-conversion stage, J. Low Temp. Phys. **151**, 51 (2008).
[19] P. J. de Visser, S. A. H. de Rooij, V. Murugesan, D. J. Thoen, and J. J. A. Baselmans, Phonon-Trapping-Enhanced Energy Resolution in Superconducting Single-Photon Detectors, Phys. Rev. Applied **16**, 034051 (2021).
[20] N. Zobrist, B. H. Eom, P. Day, B. A. Mazin, S. R. Meeker, B. Bumble, H. G. LeDuc, G. Coiffard, P. Szypryt, N. Fruitwala, I. Lipartito, and C. Bockstiegel, Wide-band parametric amplifier readout and resolution of optical microwave kinetic inductance detectors, Appl. Phys. Lett. **115**, 042601 (2019).
[21] A. G. Kozorezov, J. K. Wigmore, D. Martin, P. Verhoeve, and A. Peacock, Electron energy down-conversion in thin superconducting films, Phys. Rev. B **75**, 094513 (2007).
[22] N. Zobrist, N. Klimovich, B. Ho Eom, G. Coiffard, M. Daal, N. Swimmer, S. Steiger, B. Bumble, H. G. LeDuc, P. Day, and B. A. Mazin, Improving the dynamic range of single photon counting kinetic inductance detectors, J. Astron. Telesc. Instrum. Syst. **7**, 010501 (2021).
[23] G. Coiffard, M. Daal, N. Zobrist, N. Swimmer, S. Steiger, B. Bumble, and B. A. Mazin, Characterization of sputtered hafnium thin films for high quality factor microwave kinetic inductance detectors, Supercond. Sci. Technol. **33**, 07LT02 (2020).

[24] H. Ehrenreich, H. R. Philipp, and B. Segall, Optical properties of aluminum, Phys. Rev. **132**, 1918 (1963).
[25] See Supplemental Material at http://link.aps.org/supplemental/10.1103/PhysRevLett.129.017701 for details on the fabrication, resolving power measurement, proximity effect, quasiparticle lifetime, and calculations of the expected phonon transmission, escape time, and trapping improvement.
[26] J. W. Fowler, B. K. Alpert, W. B. Doriese, Y. I. Joe, G. C. O'Neil, J. N. Ullom, and D. S. Swetz, The practice of pulse processing, J. Low Temp. Phys. **184**, 374 (2016).
[27] L. J. Swenson, P. K. Day, B. H. Eom, H. G. Leduc, N. Llombart, C. M. McKenney, O. Noroozian, and J. Zmuidzinas, Operation of a titanium nitride superconducting microresonator detector in the nonlinear regime, J. Appl. Phys. **113**, 104501 (2013).
[28] W. A. Little, The transport of heat between dissimilar solids at low temperatures, Can. J. Phys. **37**, 334 (1959).
[29] S. B. Kaplan, Acoustic matching of superconducting films to substrates, J. Low Temp. Phys. **37**, 343 (1979).
[30] X. Qi, X. Wang, T. Chen, and B. Li, Experimental and first-principles studies on the elastic properties of α-hafnium metal under pressure, J. Appl. Phys. **119**, 125109 (2016).
[31] G. Destgeer, J. H. Jung, J. Park, H. Ahmed, K. Park, R. Ahmad, and H. J. Sung, Acoustic impedance-based manipulation of elastic microspheres using travelling surface acoustic waves, RSC Adv. **7**, 22524 (2017).
[32] M. R. Vissers, M. P. Weides, J. S. Kline, M. Sandberg, and D. P. Pappas, Identifying capacitive and inductive loss in lumped element superconducting hybrid titanium nitride/aluminum resonators, Appl. Phys. Lett. **101**, 022601 (2012).
[33] W. L. McMillan, Transition temperature of strong-coupled superconductors, Phys. Rev. **167**, 331 (1968).
[34] E. Dechaumphai, D. Lu, J. J. Kan, J. Moon, E. E. Fullerton, Z. Liu, and R. Chen, Ultralow thermal conductivity of multilayers with highly dissimilar Debye temperatures, Nano Lett. **14**, 2448 (2014).
[35] A. Giri and P. E. Hopkins, A review of experimental and computational advances in thermal boundary conductance and nanoscale thermal transport across solid interfaces, Adv. Funct. Mater. **30**, 1903857 (2020).
[36] R. D. Chaudhari and J. B. Brown, Critical currents in superconducting films of indium, Phys. Rev. **139**, A1482 (1965).
[37] S. Zhao, D. J. Goldie, S. Withington, and C. N. Thomas, Exploring the performance of thin-film superconducting multilayers as kinetic inductance detectors for low-frequency detection, Supercond. Sci. Technol. **31**, 015007 (2018).
[38] J. M. Martinis, G. C. Hilton, K. D. Irwin, and D. A. Wollman, Calculation of TC in a normal-superconductor bilayer using the microscopic-based Usadel theory, Nucl. Instrum. Methods Phys. Res., Sect. A **444**, 23 (2000).
[39] A. Fyhrie, J. Glenn, P. Day, H. G. LeDuc, J. Zmuidzinas, and C. M. McKenney, Progress towards ultra sensitive KIDs for future far-infrared missions: A focus on recombination times, in *Proc. SPIE 10708, Millimeter, Submillimeter, and Far-Infrared Detectors and Instrumentation for Astronomy IX, 10708*, edited by J. Zmuidzinas and J.-R. Gao (2018), p. 107083A, 10.1117/12.2312867.
[40] S. Kraft, A. J. Peacock, M. Bavdaz, B. Castelletto, B. Collaudin, D. Perez, R. Venn, and T. E. Harper, Use of hafnium-based superconducting tunnel junctions as high-resolution spectrometers for x-ray astronomy, in *Proc. SPIE 3445, EUV, X-Ray, and Gamma-Ray Instrumentation for Astronomy IX*, edited by O. H. W. Siegmund and M. A. Gummin (1998), Vol. 3445, pp. 226–235, 10.1117/12.330280.
[41] S. B. Kaplan, C. C. Chi, D. N. Langenberg, J. J. Chang, S. Jafarey, and D. J. Scalapino, Quasiparticle and phonon lifetimes in superconductors, Phys. Rev. B **14**, 4854 (1976).
[42] M. Baryakhtar, J. Huang, and R. Lasenby, Axion and hidden photon dark matter detection with multilayer optical haloscopes, Phys. Rev. D **98**, 035006 (2018).
[43] K. Karatsu, A. Endo, J. Bueno, P. J. de Visser, R. Barends, D. J. Thoen, V. Murugesan, N. Tomita, and J. J. A. Baselmans, Mitigation of cosmic ray effect on microwave kinetic inductance detector arrays, Appl. Phys. Lett. **114**, 032601 (2019).
[44] A. P. Vepsäläinen, A. H. Karamlou, J. L. Orrell, A. S. Dogra, B. Loer, F. Vasconcelos, D. K. Kim, A. J. Melville, B. M. Niedzielski, J. L. Yoder, S. Gustavsson, J. A. Formaggio, B. A. VanDevender, and W. D. Oliver, Impact of ionizing radiation on superconducting qubit coherence, Nature (London) **584**, 551 (2020).
[45] J. M. Martinis, Saving superconducting quantum processors from decay and correlated errors generated by gamma and cosmic rays, npj Quantum Inf. **7**, 90 (2021).
[46] M. McEwen *et al.*, Resolving catastrophic error bursts from cosmic rays in large arrays of superconducting qubits, Nat. Phys. **18**, 107 (2022).